

Interpretive approach to collective effects of electrons in multicenter problems

F. Despa and R.S. Berry^a

Department of Chemistry, The University of Chicago, Chicago, Illinois 60637, USA

Received 10 September 2002

Published online 3 July 2003 – © EDP Sciences, Società Italiana di Fisica, Springer-Verlag 2003

Abstract. Interpretive theoretical tools prove valuable in guiding the analysis of experiments in the realm of atomic clusters. Here, we review basic elements of an analytic approach that makes it possible to find and visualize the effective electrostatic potential and Coulomb correlations in multicenter problems. To illustrate the utility of these concepts we apply them to exploring molecular-doped metallic clusters. This study is aiming at a systematic, visual assessment of changes induced in screening, Coulomb correlation and effective potential by varying the charge of the electronegative impurity and its position in the cluster cage.

PACS. 36.40.Cg Electronic and magnetic properties of clusters – 36.40.Gk Plasma and collective effects in clusters – 31.25.Qm Electron correlation calculations for polyatomic molecules

In a cluster, the energy of interaction of an atom with its neighboring atoms may depend sensitively on the position of that atom in the cluster cage. It is evident that a surface atom interacts with appreciably fewer neighbors than does an interior atom. Under circumstances strictly related to the specificity of the interaction in finite systems, it follows that the location of a foreign atom doping an otherwise-homogeneous cluster can significantly affect the total energy and properties of the cluster. In other words, the structural isomers of a doped cluster involving the location of the solute relative to the host atoms have distinct energies. They may spread widely on the energy scale.

An intriguing situation seems to appear for metallic clusters in which the forces of cohesion are essentially provided by the delocalized electrons. In this case, the interactions with a foreign atom inside the cluster are screened by a mutual action of the delocalized electrons that redistribute themselves around the impurity. The perturbation of the valence electron distribution around the impurity falls off with a characteristic length that depends on the electron density. How the identity of the solute atom is still reflected in the physical properties of a doped metallic cluster is the question considered in some recent studies [1–3].

Working toward extracting insights from the probability distribution of the valence electrons, we developed recently an analytic ansatz that allows us to find and visualize the effective electrostatic potential and Coulomb correlations in multicenter problems [1]. The method adopted is a quasi-classical version of the density functional the-

ory that accounts for the electron self-distribution in the common cluster potential. While this is not at the same level of studies of electron correlations in atoms, for which very accurate wave functions have been used, it is a significant step beyond the “jellium” model, frequently invoked in describing moderately large metallic clusters [4].

Here, we review elements of the concepts and techniques employed in our approach. By using a generalized partition function for valence electrons (the Bloch density matrix), the electron self-distribution in the common potential $V(\mathbf{r})$ is derived in terms of many-body perturbation theory [5]. This approach produces the electron density $\rho(\mathbf{r})$ as a functional of $V(\mathbf{r})$

$$\rho(\mathbf{r}) = \rho_0 - \frac{k_F^2}{2\pi^3} \int d\mathbf{r}' V(\mathbf{r}') \frac{j_1(2k_F|\mathbf{r} - \mathbf{r}'|)}{|\mathbf{r} - \mathbf{r}'|^2}, \quad (1)$$

where k_F is the Fermi wavevector, ρ_0 is the free-particle density, $\rho_0 = k_F^3/3\pi^2$, and $j_1(x)$ is the first-order spherical Bessel function. Equation (1) is valid for describing metallic systems, *i.e.* systems with a high-density valence electron gas. Under conditions stipulated in reference [1], we can use the Thomas-Fermi approximation here to obtain, after a straightforward integration,

$$\rho(\mathbf{r}) = \rho_0 - \frac{q_0^2}{4\pi} V(\mathbf{r}), \quad (2)$$

where $q_0^2 = 4k_F/\pi a_H$, with a_H the Bohr radius. The results are not strongly affected by this approximation. For example, good agreement within natural limits has been obtained previously [6] for the fullerene molecule described in this way and without the simplifying linearization.

^a e-mail: berry@uchicago.edu

At the same time, we can see that the density follows the potential closely, which means that the validity of the theory is ensured, as we already mentioned above, by an appropriate constraint on the electron density. Of course this approximate theoretical model loses its validity at large distances from the ion locations because the electron density vanishes, and at very short distances, towards the center of the cluster cage, where the density becomes infinite with the potential used here.

Further, inside the electron gas of density $\rho(\mathbf{r})$, we introduce the cluster cage formed by the positive ion cores with the spatial distribution given by $\rho_+(\mathbf{R}_i)$, and apply Poisson's equation to the cluster as a whole:

$$\Delta V = 4\pi\rho_0 - q_0^2 V(\mathbf{r}) - 4\pi \sum_i^N z_i \delta(\mathbf{r} - \mathbf{R}_i). \quad (3)$$

We have to solve a self-consistent field problem that accounts for the electron distribution profile in the presence of a discrete positive background. The last term on the right side of equation (3) represents the density of positive charge with R_i the average distance of an ion from the center of the cluster and i is an index running over the ions, each with electric charge z_i . These locations are chosen without regard to the stability of the configuration.

The self-consistent solution of this equation (subject to appropriate boundary conditions, as described in Ref. [1]) gives the collective description of the cluster constituents, electrons plus ions. The total effective Coulomb potential inside the cluster is

$$\begin{aligned} V_{in} = & \frac{4\pi}{q_0^2} \rho_0 + \frac{A_{00}}{r} \sin(q_0 r) \\ & + \frac{1}{2\pi^2} \sum_{i=1}^N z_i \int d\mathbf{k} \frac{\exp[i\mathbf{k}(\mathbf{r} - \mathbf{R}_i)]}{k^2 - q_0^2} \\ & + \sum_{lm}^l \sum_{j=0}^l \frac{C_{lj}(-1)^j}{q_0^j r^{j+1}} A_{lm} \left[\exp(q_0 r) \right. \\ & \left. + (-1)^{l-j} \exp(-q_0 r) \right] Y_{lm}(\theta, \varphi), \quad (4) \end{aligned}$$

everywhere except at $\mathbf{r} = \mathbf{R}_i$. The coefficients A_{lm} must be determined. Outside the cluster, a Laplace equation applies and the solution vanishing at infinity is, with new coefficients B_{lm} ,

$$V_{out} = \frac{B_{00}}{r} + \sum_{lm}^l \frac{B_{lm}}{r^{l+1}} Y_{lm}(\theta, \varphi). \quad (5)$$

If the potential is specified on the surface of a bounding sphere (which has to contain most of the valence electron density [1]), the coefficients entering (4) and (5) can be determined by evaluating $V(R, \theta, \varphi)$ and using

$$A_{lm} = \int d\Omega Y_{lm}^*(\theta, \varphi) g(\theta, \varphi), \quad (6)$$

where $g(\theta, \varphi)$ is an arbitrary function. Here, g represents a ‘‘pseudo-charge density’’ designed to be a smooth, nodeless function which, in order to maintain the electrical

neutrality of the entire system, has to agree exactly with the true charge density outside the region bounded by the super-sphere of radius R .

This generalization of the Coulomb interaction results in a superposition of quantum oscillations given by long-range contributions and screening on the smooth ‘‘semi-classical’’ potential. In our previous report [1], we focused on their interpretive aspects and specifically on extracting insights regarding the geometric effects of Coulomb correlations for any given spatial disposition of ionic cores. Also, we explored the case of a foreign metal atom doping an otherwise-homogeneous cluster of metal atoms. The approach, which has briefly been presented here, provides us with a direct visualization of the way both the screening effect and the Coulomb correlations change with changes of the location of the impurity. This analysis is important in the context of recent observations of the role played by composition and geometry in changing the physical properties of metallic clusters [3, 7, 8].

It is to be expected that a study in the manner presented above of the case in which the impurity has an electronegative character may also bring interesting results. This investigation is motivated by current developments in the topic of molecular-doped metallic clusters [2, 9]. Apparently, the molecular core segregated around the electronegative impurity triggers a quantum size effect that leads to a rescaling of the electron density and Fermi level in the metallic shell of the cluster [2, 10]. Therefore the present study is aiming at a systematic, visual assessment of changes induced in screening, Coulomb correlation and effective potential by variations of the charge of the electronegative impurity in the molecular core.

We first recall our previous results for a metallic cluster M_{13} with icosahedral symmetry. The ionic cores were considered hard-spheres occupying a total volume in space equal to Ω_{ions} . The unperturbed density of delocalized electrons, ρ_0 , was expressed by

$$\rho_0 = \frac{3}{4\pi r_s} = \frac{N}{4\pi R^3/3 - \Omega_{ions}}, \quad (7)$$

where r_s is a point in the space available to the electrons, the ‘‘electronic interspace’’, outside the ion cores. This means that we had subtracted from the entire volume of the super-sphere of radius R the volume assigned to the ionic cores Ω_{ions} ; N is the total number of the delocalized electrons, equal to the number of ionic charges. The distance between the centers of the central and outer ions is the bond length. For numerical calculation we set $R_i = 5.9$ a.u. The core volume Ω_{ions} was computed by taking into account the ionic radius. We considered this radius equal to 2.74 a.u. so the resulting volume Ω_{ions} was 1122 (a.u.)³. For this example, the electronic interspace was chosen to be $r_s = 0.75$ a.u., in accordance with the high-density electron gas requirement ($r_s \ll 1$), and by imposing that 95% of the total electrons must be inside the super-sphere, the super-sphere radius becomes $R = 6.5$ a.u. In Figure 1 we can see the corresponding effective potential inside the super-sphere as a function of r and θ . This picture shows the regular, collective characteristics of the valence electrons we discussed above.

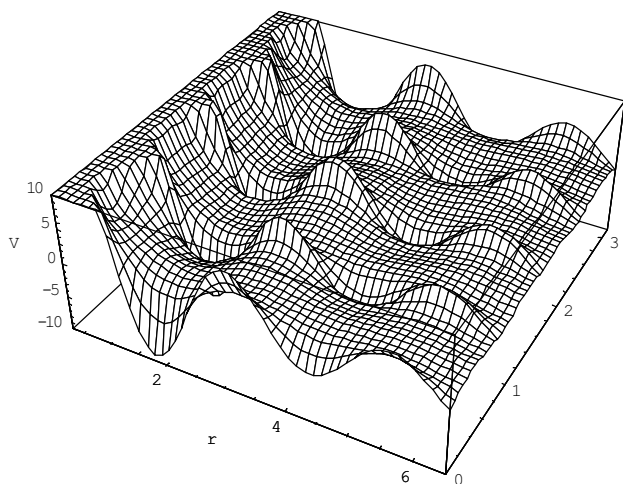


Fig. 1. The effective electrostatic potential inside the cluster cage for M_{13} for $0 < r < 6.5$ a.u., $0 < \theta < \pi$ rad and $\varphi = 0$. The right axis, from 0 to just over 3, denotes the angle θ , from 0 to π .

The oscillations we observe are a manifestation of the self-consistency of Poisson's equation and represents the main correlation effect of the electron gas in the metallic state (the high-density limit).

We have shown that [1], despite the collective aspects which contribute to the mean-field character of the effective potential, $V(\mathbf{r})$ remains sensitive to the geometry and composition of the cluster. If, for example, one host atom in the cluster cage is replaced by an impurity atom A , the potential reflects this structural change. Here, we re-explore this property for the archetypal case of the impurity A being an electronegative atom. Evidence reveals that the electronegative dopant localizes an appropriate number of host atoms (according to the stoichiometry rule) forming a “molecular” part inside the cluster [2,9,10]. Subsequently, a reduced number of valence electrons remains to be shared by the M metal ions. In the following, we consider A a divalent impurity located at the center of the cluster. For simplicity, we take the core volume of this cluster to be the same as the $13M$ ions. Figure 2a shows the corresponding effective electrostatic potential for the $(AM_2)M_{10}$ system. By comparing this with the effective mean-field potential for M_{13} , we observe that the presence of the electronegative atom at the center changes the topography of the potential surface significantly. The potential becomes more bumpy at the center, which means that the molecular core acts as a barrier for the remaining valence electrons constrained to move in the outer metallic shell. The confinement of the electrons in the outer shell induces also changes in the amplitudes of quantum oscillations relative to the previous case. The screening among the electric charges is affected by the rescaling of the electron density.

If we move the impurity to the outer shell, the disturbance due to the localization of electrons involved in screening goes toward the surface while the density peak of the delocalized electrons shifts inward. (See Fig. 2b and guide the eye along the r coordinate, from the ori-

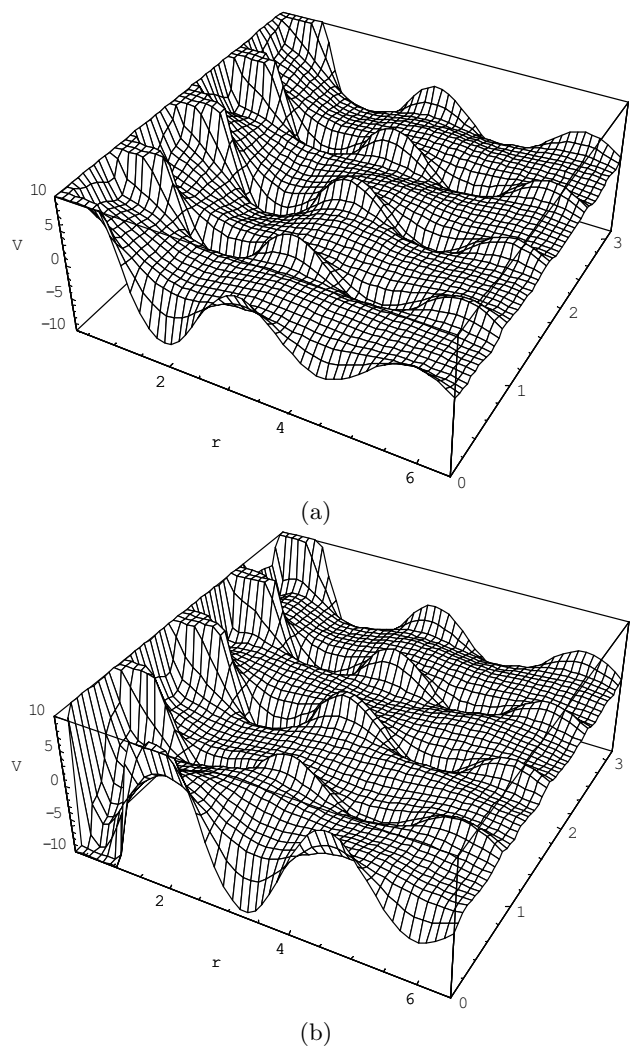


Fig. 2. (a) The corresponding effective electrostatic potential for $(AM_2)M_{10}$ system for $0 < r < 6.5$ a.u., $0 < \theta < \pi$ rad and $\varphi = 0$ with a divalent electronegative impurity in the center of the icosahedral cluster cage. (b) A plot analogous to that of (a), for the $(AM_2)M_{10}$ system with impurity at the vertex, ($\theta = 0$, $\varphi = 0$) and for $0 < r < 6.5$ a.u.

gin towards the position of the impurity of coordinates $r = 5.9$, $\theta = 0$.) This behavior of the effective potential is supplemented by the appearance of more pronounced Coulombic correlations of the valence electrons near the impurity. The disturbance of Coulomb correlations appears as irregular behavior along the θ coordinate at constant r . Also, a substantial potential difference, about 3 a.u., can be seen in Figure 2b between the position of the electronegative impurity ($\theta = 0$, $\varphi = 0$) and the antipodal position ($\theta = \pi$, $\varphi = 0$) occupied by a host ion.

Generally, the same sort of dissimilarities can be noticed in Figures 3a and 3b. Here, the impurity A is assumed to carry four negative electric charges. From these figures we can infer the change of the cluster potential due to relocation of the impurity from the center of the cluster (Fig. 3a) to the surface (Fig. 3b). Qualitatively, the effective potential, Coulomb correlations and screening have

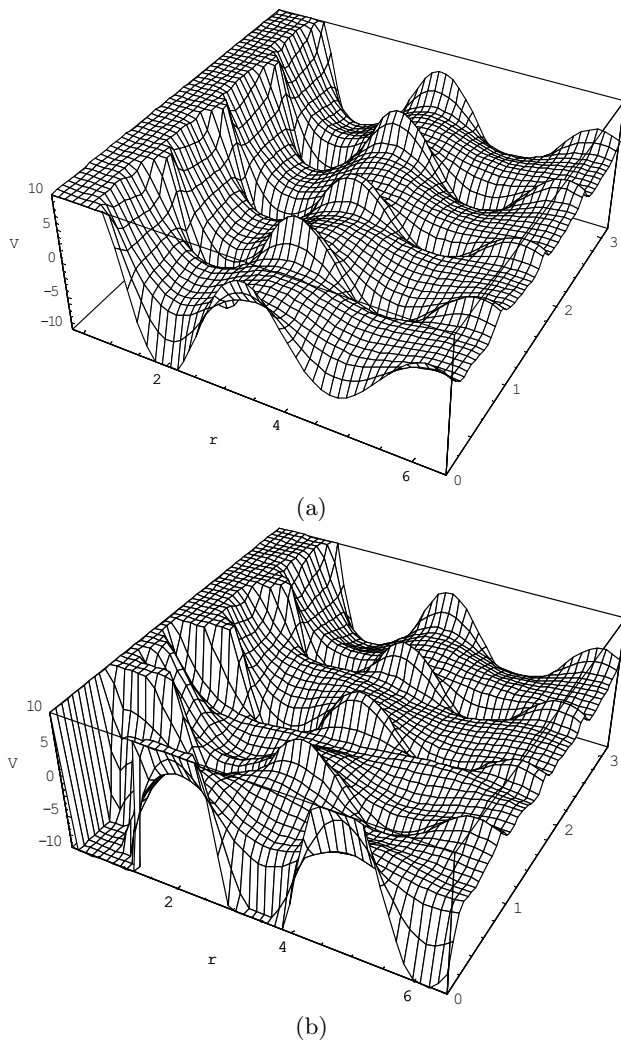


Fig. 3. (a) The effective electrostatic potential for $(AM_4)M_8$ system for $0 < r < 6.5$ a.u., $0 < \theta < \pi$ rad and $\varphi = 0$ with a tetraivalent electronegative impurity in the center of the icosahedral cluster cage. (b) The $r - \theta$ spatial dependence of the effective electrostatic potential for $(AM_4)M_8$ system with impurity at the position of the outermost ion shell.

the same behavior as above. However the range of variation of the cluster potential along the radial coordinate and the amplitude of quantum oscillations, as well, are quite different.

Because the effective cluster potential scales in its own way, repositioning the impurity may, in turn, alter the ordering of the related electron shells, a phenomenon that has been observed in many experiments [2,9,10]. There is a large variety of models explaining the shell inversions for doped metallic clusters (see references in [1,3]) and our findings may be interpreted as a qualitative support for these models. For example, in the frame of the phenomenological cluster shell models, the alteration of the electron levels from $2s-1d-2f$ to $1d-2s-1f$ arises when the shape of the potential changes from a harmonic-oscillator-like potential towards a wine-bottle-like shape. Such a change of the cluster potential can be caused for instance by re-

moving an impurity from the center of the cluster towards the surface, as we have shown previously [1]. Apparently, this is the experimental situation described in reference [3] where the shell inversion induced by Y^{3+} doping gold clusters has been interpreted in terms of a structural effect.

As we can see, the potentials in Figures 2 and 3 display barriers around the impurity that prevent the delocalized electrons from moving freely throughout the entire bulk volume. This observation is in agreement with the common picture of the “quantum size effect” [10]. It may also be interpreted as qualitative support for using a “muffin-tin” potential for a fast check of the physical properties of molecular-doped metallic clusters [2].

The method we reviewed here is simple and flexible and can yield, to some extent, accurate approximations to the exact effective potentials with minor computing effort. Also, it has the advantage of physical immediacy, *i.e.*, the present approach is easy to interpret. Presently, such an interpretative theoretical tool may provide a valuable way of guiding the analysis of experiment in the realm of atomic clusters.

The authors would like to acknowledge the support of the National Science Foundation for this research.

References

1. F. Despa, R.S. Berry, *Phys. Chem. Chem. Phys.* **4**, 3774 (2002)
2. F. Despa, W. Bouwen, F. Vanhoutte, P. Lievens, R.E. Silverans, *Eur. Phys. J. D* **11**, 403 (2000); F. Despa, *Phys. Lett. A* **276**, 109 (2000)
3. W. Bouwen, F. Vanhoutte, F. Despa, S. Bouckaert, S. Neukermans, L. Theil Kuhn, H. Weidele, P. Lievens, R.E. Silverans, *Chem. Phys. Lett.* **314**, 227 (1999); W. Bouwen, P. Thoen, F. Vanhoutte, S. Bouckaert, F. Despa, H. Weidele, R.E. Silverans, P. Lievens, *Rev. Sci. Instrum.* **71**, 54 (2000)
4. M. Brack, *Rev. Mod. Phys.* **65**, 677 (1993)
5. N.H. March, W.H. Young, S. Sampantnar, in *The Many-Body Problem in Quantum Mechanics* (New York, Dover, 1995)
6. F. Despa, *Phys. Rev. B* **57**, 7335 (1998); *Fullerenes Sci. Techn.* **7**, 49 (1999)
7. M. Heinebrodt, N. Malinowski, F. Tast, W. Branz, I.M.L. Billas, T.P. Martin, *J. Chem. Phys.* **110**, 9915 (1999)
8. J. Akola, M. Manninen, H. Hakkinen, U. Landman, X. Li, L.S. Wang, *Phys. Rev. B* **60**, 11297 (1999)
9. T. Bergmann, H. Limberger, T.P. Martin, *Phys. Rev. Lett.* **60**, 1767 (1988); H. Limberger, T.P. Martin, *J. Chem. Phys.* **90**, 2979 (1989); G. Rajagopal, R.N. Barnett, U. Landman, *Phys. Rev. Lett.* **67**, 727 (1991); P. Weis, C. Ochsenfeld, R. Ahlrichs, M.M. Kappes, *J. Chem. Phys.* **92**, 2553 (1992); C. Bréchnignac, Ph. Cahuzac, F. Carlier, M. de Frutos, J. Leygnier, J.Ph. Roux, *J. Chem. Phys.* **99**, 6348 (1993); C. Bréchnignac, Ph. Cahuzac, M. de Frutos, P. Garnier, *Z. Phys. D* **42**, 303 (1997); P. Lievens, P. Thoen, S. Bouckaert, W. Bouwen, F. Vanhoutte, H. Weidele, R.E. Silverans, A. Navarro-Vázquez, P.V.R. Schleyer, *J. Chem. Phys.* **110**, 10316 (1999)
10. H. Limberger, T.P. Martin, *J. Chem. Phys.* **90**, 2979 (1989)